X-ray studies of high-temperature defects in concentrated isotopic helium solid solutions

B. A. Fraass* and R. O. Simmons
Department of Physics and Materials Research Laboratory, University of Illinois at Urbana-Champaign, 1110 West Green Street, Urbana, Illinois 61801
(Received 5 August 1987)

Vacancy concentrations in bcc crystals of helium isotope mixtures of nominal composition 12%, 28%, and 51% ^{3}He have been inferred from measurements of temperature dependence of x-ray lattice parameter, a, in samples confined at several different constant macroscopic volumes. The data have been parametrized by an activated form, and in each case some possible separation of the free energy into energy and entropy contributions is discussed. The results for each composition are different, yet certain patterns can be discerned, such as the likelihood of significant vacancy-solute binding. Estimates of the vacancy free volume of formation are obtained for the 28% and 51% ^{3}He mixtures. In low-density 51% crystals the changes in $3\Delta a/a$ are extraordinarily large, up to 5% near melting. The situation is reminiscent of CsCl-structure alloys, except that those alloys show ordering at all temperatures, whereas helium mixtures show isotopic phase separation at low temperatures.

I. INTRODUCTION

Thermal defect studies in the solid heliums have so far mostly been carried out in pure ^{3}He or ^{4}He specimens, or in ^{4}He samples containing, at most, a few percent ^{3}He used as an NMR probe. Ultrasonic and pressure techniques have also provided sensitive, albeit indirect, evidence about thermally activated defects in various solid heliums. It has been established by NMR, for example, that in low-density bcc solid ^{3}He-^{4}He mixtures there are extraordinary atomic diffusivities, up to 2×10^{-7} (cm^2/s),[1,2] corresponding to unusual delocalization of atoms about the atomic sites.[3] As another example, in a predominantly ^{4}He matrix, ^{3}He-^{4}He binding effects are measurable and various tunneling processes have been identified.[4]

When results from these methods are analyzed along with direct x-ray measurements of vacancy content,[5-7] a considerable amount of information is available in the pure solids. Among the information is the following: (a) for thermal vacancies in bcc ^{3}He, the vacancy free energy f and the self-diffusion activation energy agree, so vacancies apparently move by a tunneling mechanism; (b) vacancy free volumes of formation in bcc ^{3}He are somewhat less than 0.4 atomic volume, a magnitude in agreement with expectation based upon bulk elastic properties, and the corresponding vacancy-formation pressure can be deduced; (c) in bcc ^{3}He and bcc ^{4}He the ratio f/T_m is about 5, over a large range of melting temperatures, T_m, differing by a factor 4; that is, the vacancy content in bcc solid heliums at melting is about constant over that range of T_m's.

The present work was undertaken to explore what x-ray methods can contribute to understanding of defect effects in concentrated solid isotopic solutions of ^{3}He and ^{4}He. In this system there are considerable ranges of compositions, of molar volumes, and of corresponding melting temperatures available for such exploration. In solid helium solutions, equilibration is greatly assisted by high intrinsic atomic mobilities, so that future detailed studies, especially when carried out with simultaneous measurements of other physical parameters, such as pressure, should be possible in reasonable time scales for specimens with large molar volumes. On the other hand, at small molar volumes ($\sim$20 cm^3), the relaxation time is much extended.[8,9]

Present x-ray results include three ^{3}He-^{4}He compositions and several fixed macroscopic molar volumes. These already yield some qualitatively new and surprising features. Notable is the finding of very large lattice parameter changes over large temperature ranges up to melting. If one assumes these to be thermally generated point defects, the corresponding thermal vacancy concentrations are reminiscent of phenomena which occur in ordered bcc CsCl-type alloys.[10] Concurrently, because suitable x-ray specimens are laborious to prepare and characterize, we studied the phenomenon of isotopic phase separation at low temperatures; the results of that study are reported separately.[11]

II. VACANCIES IN CONCENTRATED MIXTURES

To show elements which may come into account in the equilibrium of localized point defects, we first recapitulate the usual thermodynamic results for monovacancies.[6,12] Their number n_{1v} in a crystal of N like atoms (their concentration c_{1v}) is

$$c_{1v}=\frac{n_{1v}}{N+n_{1v}}=\exp(-f_{1v}/k_BT)=\exp(-e_{1v}/k_BT+s_{1v}/k)\,, \quad (1)$$

where f_{1v}, e_{1v}, and s_{1v} are the free energy, the energy, and nonconfigurational entropy of formation, respectively (k_B is the Boltzmann constant). In a specimen at constant volume, the pressure of formation is

$$P_{1v} = -\left[\partial f_{1v}/\partial V\right]_T = \frac{v_{1v} B_T}{V} , \tag{2}$$

where v_{1v} is the free volume of formation and B_T the isothermal bulk modulus.

Even in a one-component host there may be vacancy binding. It is convenient to define this relative to the monovacancy energy as

$$e_{jv} = j e_{1v} - e_{jb} , \tag{3}$$

where a cluster of j vacancies has binding energy e_{jb}. The total concentration of vacant atomic sites, in the presence of binding, is[13]

$$\Delta N/N = j\, c_{jv} = A_{jv} (c_{1v})^j \exp(e_{jb}/k_B T) , \tag{4}$$

when the cluster entropies are ignored and A_{jv} is a constant geometrical factor that depends on the number of ways the cluster of j vacancies can be oriented in the lattice ($A_{2v} = 4$ for a bcc lattice).

Further, in a disordered solvent-solute mixture the vacancies may be "free" of the influence of the solute atoms or be "bound" to one.[14] If there are N solvent atoms, N_s solute atoms, n free vacancies, and $N_s p$ solute-vacancy bound states (s-v's), then the free energy of the crystal is

$$F = F^0 + nf + N_s p\,(f - f_b) - T \ln(W) , \tag{5}$$

where F^0 is the free energy of the hypothetical vacancy-free crystal, f is the free-vacancy-formation energy, f_b is the s-v binding free energy, and W is the configurational term. n and p are determined by minimizing the free energy:

$$\frac{\partial F}{\partial n} = 0 = \frac{\partial F}{\partial p} . \tag{6}$$

The difficulty is that W is complicated. In a nearest-neighbor model it can be expressed as a product:

$$W = ABC . \tag{7}$$

A is the number of ways of arranging $N_i p$ s-v's on N_s sites:

$$A = \frac{(z)^{N_i p}}{(N_i p)!} \prod_{s=0}^{N_i p - 1} (N + N_i + N_i p + n - 2s) , \tag{8}$$

where z is the number of nearest neighbors ($z = 8$ for bcc). B and C are, respectively, the number of ways of putting the $N_i(1-p)$ free solute atoms, and the n free vacancies, on the lattice without either having a near neighbor of the other or of the s-v's already on the lattice.

$$B = \frac{[N + N_i(1-p) + n]!}{[N_i(1-p)]!(N+n)!} , \tag{9}$$

$$C = \frac{[N - zN_i(1-p) + n]!}{[N - zN_i(1-p)]! n!} . \tag{10}$$

The difficulty for concentrated solutions is obvious.

For the extremely dilute case, one finds,[15] for the total vacancy concentration,

$$\exp(-f/k_B T)[1 - zN_i + zN_i \exp(f_b/k_B T)] , \tag{11}$$

a result which has intuitive interpretation, but unfortunately only a very limited domain of applicability.

When the host has two components, such as ^{3}He and ^{4}He, vacancies may bind preferentially to one of them. A naive argument goes as follows: At a given pressure the molar volume of ^{3}He is larger than that of ^{4}He, because of its higher zero-point kinetic energy; ^{3}He atoms in a mixed lattice will therefore be somewhat compressed; this compression can be relieved next to a vacancy; a ^{3}He-vacancy binding energy thus results. This naive picture is oversimplified. For example, Locke and Young[16] present an argument that formation of this bound state will localize the vacancy, thereby raising its energy. The magnitude of this effect is, however, unknown at present because the extent of delocalization is unknown.[6] The concentration of vacancies in bcc ^{3}He does not seem changed, within the sensitivity of direct measurements,[17] by the addition of 1% of ^{4}He.

The situation when the mixed crystal has about equal numbers of two constituents, and these form an ordered $B2$ lattice, has been summarized by Kim.[18] Again, a model is used based on nearest-neighbor bond-energy approximation. The number of bonds of energy e_{kl} is labeled n_{kl}. For atoms labeled A and B, the configurational free energy is

$$F = -n_{AA} e_{AA} - n_{BB} e_{BB} - n_{AB} e_{AB} - k_B T \ln\left[\frac{(N+n)!}{N_{Aa}! N_{Ba}! N_{va}!} \frac{(N+n)!}{N_{Ab}! N_{Bb}! N_{vb}!}\right] . \tag{12}$$

Here, the ordered sublattice of the A's is denoted by a, the numbers of A atoms on that sublattice by N_{Aa}, N_{vb} is the number of vacant B-atom sites, etc. A measure of the ordering energy in such a crystal is

$$w = e_{AB} - \tfrac{1}{2}(e_{AA} + e_{BB}) . \tag{13}$$

In helium isotope mixtures at low temperature, w is positive since isotopic phase separation occurs.[11,19] Nevertheless, let us consider further some properties of this model.

One proceeds by expressing the free energy F as a function of n, N_{Ab}, and N_{Bb} (noting that $N_{Aa} = N - N_{Ab}$, $N_{Bb} = N - N_{Ba}$, $N_{va} = n + N_{Aa} - N_{Bb}$, and $N_{vb} = n - N_{Ab} + N_{Bb}$). This free energy is minimized with respect to these three independent variables. One then obtains, for example,

$$\frac{N_{va}}{N+n} = \left[\frac{N_{Aa} N_{Ba}}{N_{Ab} N_{Bb}}\right]^{1/4} \exp[-4(e_{BB} - w)/k_B T] , \tag{14}$$

a similar expression for N_{vb} with e_{AA} in the exponential factor, and more complicated expressions for N_{Ab} and N_{Ba}. If $|e_{AA}| > |e_{BB}|$, it turns out that practically all the vacancies will be located upon a sites and the b sites will contain $\frac{1}{2} N_{va}$ "excess" antistructure A atoms; that is, approximately $N_{Ab} - N_{Ba}$ of them.

One recognizes that in a real mixture, ordering on the two sublattices may be incomplete. In the presence of the vacancies, one defines an order parameter, η, as

$$2\eta=(N_{Aa}-N_{Ba})/N-(N_{Bb}-N_{Ab})/N\ . \quad (15)$$

Kim[18] shows calculated results for NiGa (Ref. 20) with two different values of η, 0.8 and 0.9.

In both kinds of calculations described above, one should note that the configurational entropy part of the vacancy free energy varies with the order parameter, by way of the random probabilities of occurrence of local configurations. (In a pure substance, there is a constant configurational entropy for the monovacancy.) As the order parameter varies with temperature, then so will the vacancy free energy. This has been shown, for example, in the $B2$-type system β-brass.[21]

The various kinds of calculations above are not easily unified. They are sufficient, however, for discussion of the present exploratory experiments.

III. EXPERIMENTAL TECHNIQUES

A. Cryostat, dilution refrigerator, and sample cell

The rigid-tail cryostat and dilution refrigerator used in this work was designed, built, and described by Heald and Simmons.[22] The cryostat is of rigid-tail design so that (a) the sample cell stays fixed in space regardless of the levels of liquid helium and liquid nitrogen in the cryostat, and (b) there are no cryogens in the path of the x rays. The refrigerator and sample cell are shown in Fig. 1, which also shows the positions of the heaters and thermometers for the present work. The design allows careful crystal preparation and characterization and furnishes adequate time to perform absolute lattice-parameter measurements when desirable.

The pressure system and Lucite sample cell were basically unchanged from previous work on pure ^{3}He,[6] with several minor additions. The arrangement used here is shown in Fig. 2. The basis of the system is the room-temperature separator, which allows high-pressure ^{4}He to pressurize the ^{3}He-^{4}He sample with a stainless-steel bellows arrangement. The system allows both preparation of isotopic mixtures and measurement of their composition.

The Lucite cell, shown in the inset of Fig. 2, was changed from the original design because the first crystals grown (samples nos. 1–8) showed an unnerving tendency to rotate in the cylindrical sample cell, sometimes at speeds as high as 1 deg/min. To counter this problem a small (<1 mm) spike of In solder was placed on the stainless-steel fill line inside the cell. The spike destroyed the cylindrical symmetry of the cell and improved the stability of the crystals. Although the crystals still rotated, especially near the melting temperature, this rotation during a measurement sequence usually was measured in hundredths of a degrees instead of tens of degrees. The cell is stiff enough to provide a container of essentially constant macroscopic volume as the temperature (and hence the pressure) of a solid helium sample is changed.[6]

B. Temperature measurement and calibration

A change, compared to previous work,[6] was the use of germanium thermometers useful to lower temperatures, their calibration by various methods [^{3}He vapor pressure above 1 K, a cerium manganese nitrate (CMN) magnetic thermometer below 1 K, a set of National Bureau of Standards (NBS) superconducting fixed points[23]], and measurement of their resistance by a four-terminal ac bridge, with preset limitations on power dissipation in each temperature range. All temperatures quoted are from the EPT-76 temperature scale.[24]

Calibrations of secondary thermometers were performed by removing the sample cell and replacing it with

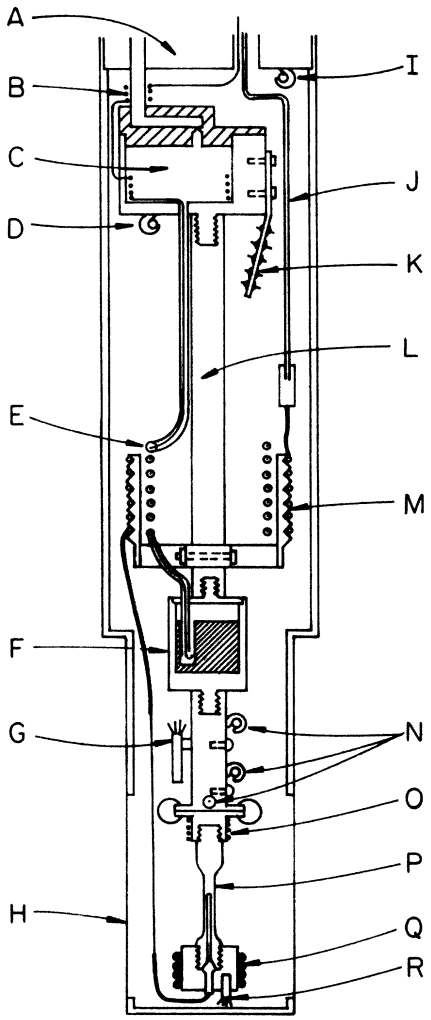

FIG. 1. Cross-sectional view of the sample chamber, including dilution refrigerator: *A*, 1-K pot; *B*, flow impedance; *C*, still; *D*, still thermometer (carbon); *E*, coaxial-tube heat exchanger; *F*, mixing chamber; *G*, germanium thermometer (reference); *H*, 12-μm aluminized Mylar x-ray window; *I*, pot thermometer (carbon); *J*, sample fill line; *K*, thermal ground for electrical leads; *L* graphite support rod; *M*, nylon support for lower sample fill line consisting of $\sim$1-m length of 0.04-cm-o.d.$\times$0.025-cm-i.d. cupronickel tubing; *N*, carbon-resistance thermometers; *O*, control heater; *P*, Lucite sample cell; *Q*, gradient heater; *R*, germanium thermometer.

a copper block in which were mounted four germanium thermometers and the NBS fixed-point device. From various cross-checks between these respective calibrations and previous ones on the reference germanium thermometer, the present temperature measurements are believed to be accurate to better than $\frac{1}{2}\%$ over the range from 40 mK to 7 K. Questions of thermal contact and of heat transport within the specimens and with their container are largely answered by concurrrent phase-separation studies at lower temperatures.[11]

C. Sample preparation and crystal growth

Successive specimen compositions were prepared by dilution of an original ^{3}He sample with ^{4}He in successive steps. This was accomplished by admitting high-pressure ^{4}He ($\sim$13 MPa) into the mixture side of the system (Fig. 2). A pressure difference (over 7 MPa) minimized the chance of contamination of the ^{4}He side with ^{3}He.

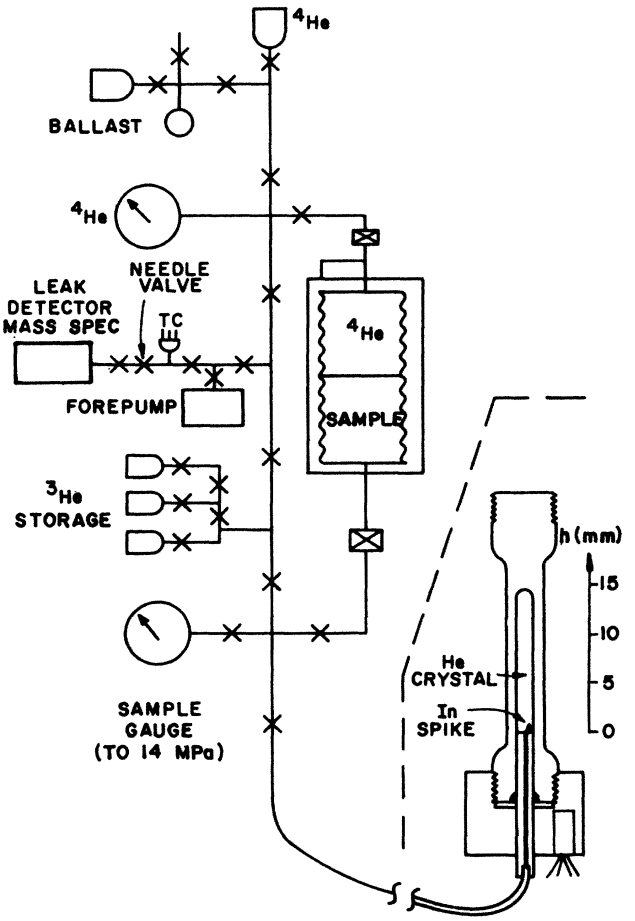

FIG. 2. Schematic of gas-handling system and sample cell. Outside the cryostat all tubing is 0.25-mm-i.d.$\times$1.6-mm-o.d. stainless steel. Sample pressure gauge is Heise model CM 4527 and ^{4}He pressure gauge is Heise CM 4526. The metal bellows-sealed separator used to pressurize the sample is shown very schematically; on either side are electrically operated solenoid valves which prevent overpressurization of the separator. The inset shows the Lucite sample cell to scale, including an In spike to minimize crystal rotation.

Homogeneity of the resulting gas mixture, which was resident both in the mixture gauge and the separator, was improved by repeated separator compression of the mixture gauge to about 9 MPa, then depressurization to about 2 MPa.

The method used here for growth of crystals has been described by Fraass and co-workers.[25] The crystals were grown slowly from the liquid at constant pressure, the fill line kept open until the growth was completed (Fig. 2). A plug in the fill line was then frozen to keep the crystal at constant macroscopic volume. The crystals grew from the top down in the cell, under a computer control which lowered the temperature of the top of the cell slowly. A growth curve was obtained by recording the temperature at the bottom of the cell as a function of time on a chart recorder. The stated melting temperature, T_m, is the nominal temperature at which the crystal finished growing.

The growth of good-quality crystals was essential. Crystal quality was first checked by taking Laue transmission photographs, then by scans using the x-ray–position-sensitive-detector (PSD) system (Sec. III E). More than 80% of the crystals grown were discarded because of insufficient size or quality. A sample of concentrated mixture which consisted of a single crystal through the whole cell could not be obtained.

Typical growth curves are shown in Fig. 3, one for each mixture concentration studied here. The curves for each concentration are qualitatively different, and different from those for isotopically pure and almost pure helium, shown also for comparison. For the latter, the beginning and end of growth are obvious, the temperature gradient during growth is fairly small, and the growth time of 0.5–2 h is easily determined. Note the differences in the mixture growth curves. It is difficult to determine T_m for the 51% mixture, and the 28% mixture is different only in degree. This is because the mixtures are nonazeotropic and thus the crystals do not grow at exactly the same concentration as that of the liquid from which they are grown. In the 12% crystals we always found a large amount of supercooling before growth begins, no matter what the cooling rate. Interestingly, for the 12% crystals, six in succession grew in the same orientation, then three more grew in the same (but different from the previous six) orientation. Similar behavior was seen by Osgood and co-workers[26] in bcc ^{4}He; all eight of their crystals had a (001) reflection within 5° of the others. Each of our six 12% crystals had a (110) reflection within 1° of the others.

D. Sample concentration analysis

The concentration of ^{3}He in the mixtures was measured with a calibrated mass-spectrometer leak detector, with an intrinsic sensitivity for the isotope ratio of about 500 ppm. The procedure involved warming the cryostat to 78 K. During the 24-h warmup the separator was used to lower the pressure in the fill line and sample cell, while the gas was saved by compressing it into the mixture gauge. Near 78 K the fill line and cell were pumped out through the leak detector, while the ratio of ^{3}He to ^{4}He

coming out was measured periodically. The gas initially pumped out is from the fill line only, so its concentration is not desired. Also not desired is that measured after the cell pressure is low because it is sensitive to the vapor pressures of any residual gases in the cell. Only the concentration of the gas pumped out between these two extremes is useful; these readings do vary somewhat, and their variability is the largest contribution to the estimated uncertainties given in Table I.

Neither the indicated starting nor finishing temperature obtained from a growth curve is a useful check on the mixture concentration, unfortunately. These temperatures are imprecisely indicated (Fig. 3). While the point at which growth starts should be on the liquidus, there is some temperature gradient in the cell during growth and the thermometer at the bottom of the cell does not give the actual temperature at which the crystal growth at the cell top begins. Also, the indicated temperatures were lower than published phase-diagram data[27–29] by as much as 0.1 deg, because of the difference in the liquidus and solidus curves. Most P-T melting-line data were obtained on the liquidus, while current T_m's are on the solidus.

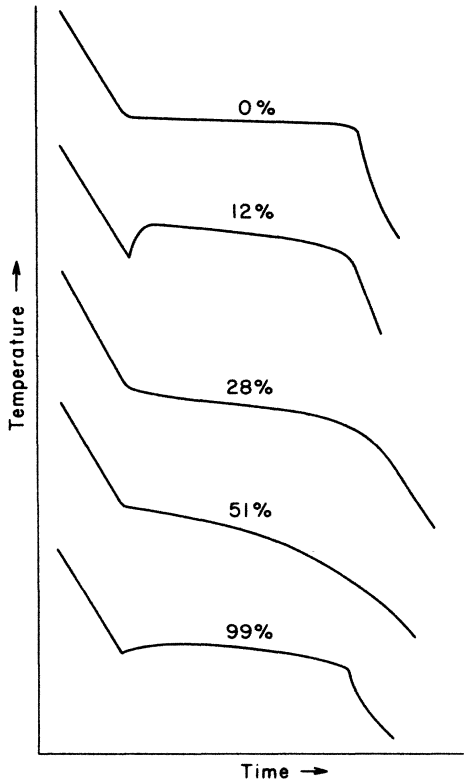

FIG. 3. Crystal-growth curves for different ^{3}He concentrations. The five curves are schematic representations of the temperature at the bottom of the sample cell plotted vs time, as the top of the cell is cooled at a constant rate. The flatter region in the center of each occurs as the crystal grows. The dip seen in the 12% mixture before the growth begins corresponds to supercooling of the liquid. A typical temperature range for the growth curves shown here is about 200 mdeg, while the extent of the time scale is typically 1–3 h.

TABLE I. Mixture concentrations. The nominal mixture, measured ^{3}He concentration (x), and the uncertainty in x are listed for the various crystals measured in this work.

Nominal mixture (%)	x	Uncertainty	Sample no.
51	0.506	0.012	20–26
28	0.280	0.005	27–28
12	0.125	0.015	29–30

E. X-ray-diffractometer–PSD procedure

The novel x-ray-diffractometer–position-sensitive-detector (PSD) system which was used in the present work is described elsewhere.[30] It consists of a three-circle goniometer, upon which are mounted as x-ray source a commercial Cu-anode x-ray tube with collimator and as detector a one-dimensional (1D) position-sensitive proportional counter. Flexible, varied, and relatively rapid scans can be performed on a single-crystal sample held fixed in position and in orientation, as in the present cryostat. For a weakly scattering sample such as the 1.6-mm-diam helium crystals of the present work, one is restricted to forward scattering. Nevertheless, relative changes in lattice parameter can be determined with a precision better than 60 ppm; absolute lattice parameters can be measured with an accuracy of about 300 ppm and with a reproducibility better than that. Further, the PSD permits efficient characterization of sample crystal mosaic, and continual monitoring of that property, while relative lattice-parameter scans are made.

Crystal growth was followed by at least several hours of annealing with the fill line unplugged. Then as the fill-line heaters were turned down, a series of transmission Laue photographs was taken, at different heights on the cell and at different polar angles. It was found that in the concentrated mixtures, the useful grain was always at the top of the cell, i.e., had been grown first. After crystal orientation and diffractometer alignment, data acquisition then commenced, usually with an absolute lattice-parameter measurement performed first. This was followed by measurements of relative changes in lattice parameter which consisted of two ω scans[30] at each successive temperature.

IV. RESULTS

Data of different sorts were obtained. Measurements of the absolute lattice parameters were made, with an accuracy of about 300 ppm. Measurements of changes in lattice parameter were made with the ω scan.[30] Together, these data have made accurate determination of lattice-parameter changes possible over a wide range of temperature in various concentrated ^{3}He-^{4}He mixtures at essentially constant macroscopic volume. They also gave values of x-ray molar volumes of the mixtures just above phase separation. Finally, analysis of changes in x-ray peak shapes, made because of phase separation occurring in the samples at low temperatures, furnished necessary independent evidence to characterize the crystals for con-

siderations of thermal reversibility. In each specimen, rather complex changes took place; because of their primary relevance to our concurrent phase-separation study, they are described in that paper.[11]

An ideal study aimed at thermal vacancies alone would avoid temperatures at which phase-separation phenomena take place. But in the present exploratory studies we judged it preferable, at the expense of some clarity in the overall data for both purposes, to cover both phase-separation and thermal defect regimes even when some irreversibility was introduced through specimen crystal substructure changes.

For the different crystals the respective data are shown in Figs. 4–10. A few comments are appropriate about certain samples. Sample no. 23 (Fig. 4) apparently had a small subgrain contributing somewhat to changes in x-ray peak shape at the base. For this case the upper 70% (rather then the usual 90%) of the peak was used to calculate the peak centroid. The data shown were obtained upon original warming. This specimen was most extensively examined, subsequently, for phase-separation signatures (changes in lattice parameter, Bragg-peak width, and mosaic spread);[11] these changes were most prominent below about 0.6 K. The total change in $3\Delta a/a$ for this 21-(cm^3/mol) 51% ^{3}He specimen was rather small, at most 0.3%.

$\Delta a/a$ data from crystal no. 24, 51% ^{3}He at much larger molar volume, were taken upon cooling (Fig. 5). The observed change in $3\Delta a/a$ is enormous, up to 3%. In the range 0.5–0.4 K, just above phase separation, the lattice parameter was observed to decrease somewhat. This sample was subsequently left for many hours below the phase-separation temperature, and the prominent diffraction feature in the region of reciprocal space examined for the separated sample near 0.2 K apparently shifted from being the ^{4}He-rich feature to the ^{3}He-rich one, with a lattice-parameter increase of over 5%, as warming began. Because of this, the sample was evidently different

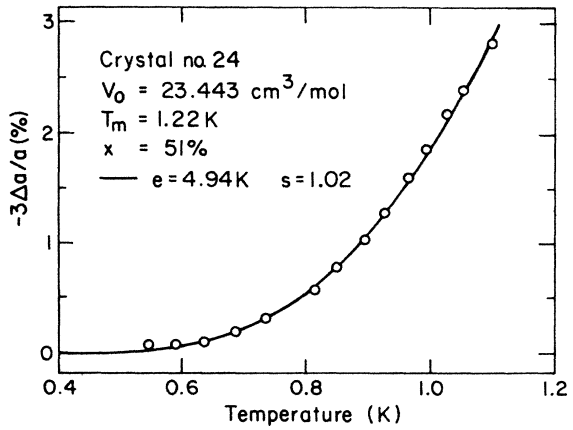

FIG. 5. Sample no. 24 data on lattice-parameter changes, obtained upon cooling. The solid line is a least-squares fit with both e and s varied. Setting $s=0$ produces a fair fit yielding $e=3.8$ K. Further cooling to phase separation at 399 mK gave an anomalous decrease in lattice parameter, not shown.

from the original one and we judged these heating measurements unsuitable for comparison with the cooling ones. It is interesting, however, that qualitative extrapolations of the cooling and warming data to the melting temperature can apparently be brought to meet at the melting temperature. [The molar volume so indicated is, perhaps coincidentally, near the value V_m calculated from Eq. (16) below.]

Another 51% crystal, no. 26, was prepared at slightly higher density, to check the surprising large lattice-parameter changes seen in sample no. 24 at high temperature. Figure 6 shows the confirmation, from cooling data. As with all the data on lattice-parameter changes reported here, two x-ray scans were taken at each temperature; these agree very well over the whole temperature ranges of these data. Near phase separation below the limits of Fig. 6, the details of Bragg-peak fragmenta-

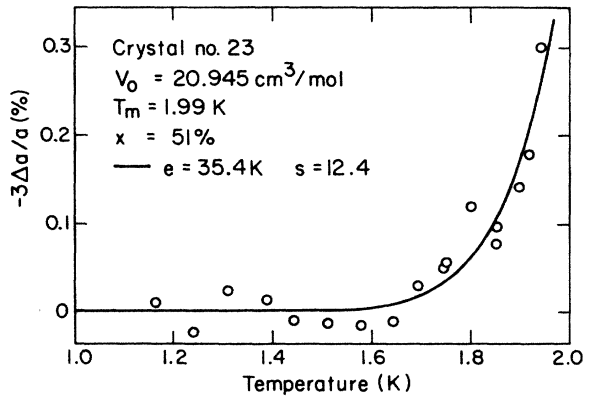

FIG. 4. Sample no. 23 measurements of lattice-parameter changes, obtained upon warming. The solid line is a least-squares fit to Eq. (17) with both e and s varied, and the reference level at low tempertures also thus determined. A much poorer fit with $s=0$ yielded $e=11.8$ K. Not shown are many other lattice-parameter data obtained at temperatures down to phase separation at 299 mK.

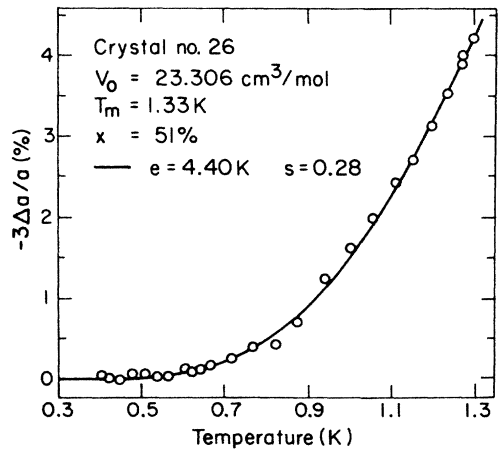

FIG. 6. Sample no. 26 data, obtained upon cooling. The solid line is a least-squares fit with both e and s varied. Setting $s=0$ produced almost as good a fit also, with $e=4.1$ K. Phase separation for this sample was at 388 mK.

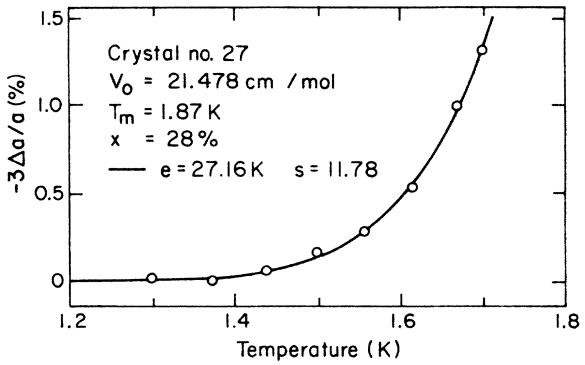

FIG. 7. Sample no. 27 measurements before phase separation, which for this sample was at 330 mK. The data were obtained upon cooling, with data below 1.25 K excluded because of entry into the mixed bcc-hcp phase. The solid line is a least-squares fit in which both e and s are varied. No reasonable fit with $s=0$ is possible.

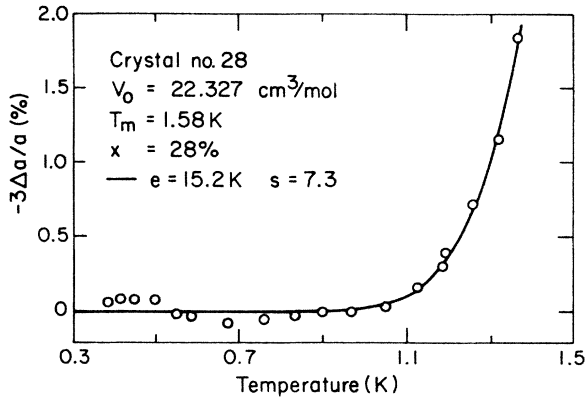

FIG. 9. Sample no. 28 measurements, obtained upon cooling. The solid line is a least-squares fit allowing both e and s to vary. With $s=0$, a poor fit is obtained with $e=5.8$ K. There is an apparent decrease in lattice parameter in the range 0.4–0.6 K, above the phase-separation temperature of 367 mK.

tion are reported elsewhere.[11] These showed that the sample, once it was again warmed above such separation, had a mosaic spread of over 5° and was structurally different from the homogeneous one for which (cooling) data are shown in Fig. 6. As for sample no. 24, the lattice-parameter data apparently converge once again at the melting temperature.

Sample no. 27, 28% ^{3}He, yielded apparently useful data both upon cooling and warming, because the specimen did not sit below the phase-separation temperature for more than about 6 h, thus minimizing the damage done to the crystal quality. For this crystal, we think that some small irreproducible variations in lattice parameter in the range 0.6–1.2 K were due to the presence of some mixed bcc-hcp phase. Differences in the fits (see below) to the cooling (Fig. 7) and the warming (Fig. 8) runs are in large part caused by the different ranges of temperature covered by the stable data. As before, near melting the post-phase-separation lattice parameter agreed with that found before phase separation.

Data on another 28% crystal, sample no. 28, prepared at lower density, are shown in Fig. 9. As for sample no. 27, some small lattice-parameter perturbations attributable to mixed hcp-bcc phases were present at intermediate temperatures, and as before there is at the end apparent agreement in lattice parameters extrapolated to melting. The sample was below the phase-separation temperature only 5 h.

Finally, studies were made on a 12% ^{3}He crystal, sample no. 29, which exhibited some time-dependent changes at intermediate temperatures which we attribute to mixed phases. This sample was only very briefly held below phase separation. Initial warming data are shown in Fig. 9. Two succeeding warming runs agreed qualita-

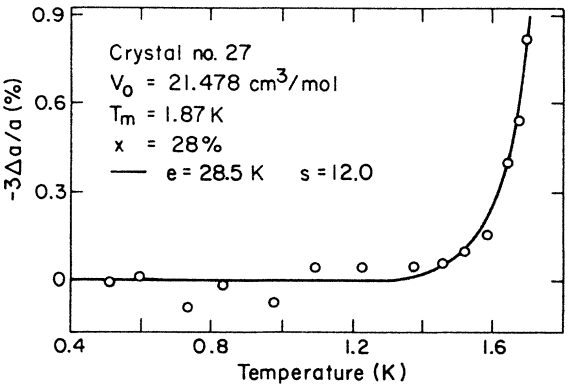

FIG. 8. Sample no. 27 measurements, obtained upon warming after the sample had been cooled into the phase-separation region. The solid line is a least-squares fit allowing both e and s to vary. Data below 1 K show additional scatter as the specimen remixes. A fit with $s=0$ yields $e=8.6$ K and represents the data very poorly above 1.4 K.

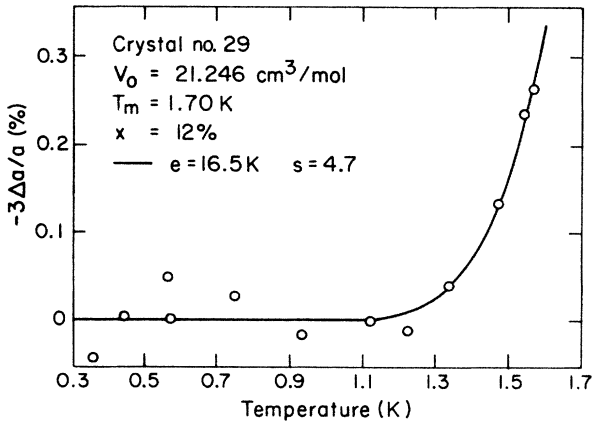

FIG. 10. Sample no. 29 measurements, obtained upon warming, after a brief period of phase separation, which for this sample was at 267 mK. The solid line is a least-squares fit allowing both e and s to vary. With $s=0$, a fair fit with $e=9.3$ K resulted. Two succeeding runs were found to agree qualitatively with this warming run.

tively with the data shown.

The results of the absolute lattice-parameter measurements on six crystals are given in Table II. These data, in conjunction with the $\Delta a/a$ measurements, were used to obtain the x-ray molar volumes of the various crystals at intermediate temperatures, V_0, also given in Table II. Shown also are molar volumes obtained from use of interpolated values of the pressure-volume-temperature (PVT) measurements of Grilly and Mills[31] in the formula

$$V(x,P)=xV_3(P)+(1-x)V_4(P)+x(1-x)c \ , \quad (16)$$

where $V_3(P)$ is the molar volume of ^{3}He at pressure P, x is the ^{3}He concentration, $V_4(P)$ is the ^{4}He molar volume, and C is a constant which Mullin[32] has calculated to be -0.4 cm^3/mol.

The characteristics of these data are summarized in Table III. This table contains the results of two parametrized fits to each data set. The first is a simple exponential fit,

$$-3\,\Delta a/a = \exp(-f/k_BT), \quad f=e-Ts \ , \quad (17)$$

with s held equal to zero. This is included for comparison with previous vacancy data on solid helium,[6,7] which are not precise enough to be used to determine more than one fitting parameter. The second fit, the last two columns in Table III, shows results of fits in which both e and s were allowed to vary. Although the results of this fit are sensitive to small variations in the data, comparison of such a fit with the $s=0$ fit shows clearly that the fit with s varying is a better parametrization of the data. These fits are shown as solid lines on Figs. 4–10. The errors quoted for both fits are only the statistical probable uncertainties calculated from each fit.

V. ANALYSIS

A. General results

Inspection of Figs. 4–10 reveals that the $s=0$ parametrization of the data by Eq. (17) is poor for all cases except possibly sample no. 26. On the other hand, fitting using only the two parameters s and e of Eq. (17) is reasonable. Probably the precision of the measurements does not by itself justify, without other considerations, any more elaborate parametrization of the results. Nevertheless, some inferences about possible applicabilities of the more elaborate models mentioned above in Sec. II can be drawn. Also, because of the inability of measurements other than those of the present type to obtain defect entropies directly, some discussion of the factor $\exp(s/k_B)$ is worthwhile.

The only published activation energies for concentrated bcc mixtures have been obtained from NMR experiments. Miyoshi and co-workers[1] have made T_1, T_2, and diffusion measurements on mixtures with $x=32.1\%$, 7.78%, and 1.94%, respectively. Spin diffusion measurements have been done by Grigor'ev and co-workers[2] in mixtures with $x=6.3$, 2.17, and 0.75%, respectively. More recent NMR studies[4] have been carried out with very small concentrations x in order to elucidate the elementary excitation and scattering phenomena.

One way to summarize the results of the present study and to compare them to previous NMR work is to take each value e (obtained from the present $s=0$ fits), reduce it by division by the respective melting temperature T_m, and plot the ratio versus the molar volume. The results are shown in Fig. 11. There is a well-marked tendency for the (reduced) e values to fall by a factor of 2 as the

TABLE II. Measured and derived characteristics of crystal samples grown at various melting pressures (P_m) and corresponding melting temperatures (T_m). The respective estimated possible errors are 8 kPa in P_m and 0.5% in T_m. The absolute bcc lattice parameters (a) measured on (110) planes at the various temperatures (T) have an estimated uncertainty of 300 ppm. Low-temperature x-ray molar volumes (V_0) have been corrected for thermal vacancy content. The molar volumes on the melting line (V_m) are estimated from Eq. (16). The estimated possible error in V_0 is 900 ppm, which corresponds to 0.019 cm^3/mol. If use of Eq. (16) is correct, the estimated possible error in V_m is about 0.5%, which corresponds to 0.1 cm^3/mol.

Sample no.	P_m (MPa)	T_m (K)	T (K)	a (Å)	V_0 (cm^3/mol)	V_m (cm^3/mol)
23	6.187	1.99	1.823	4.110 90	20.945	20.43
			1.052	4.112 10		
24	3.220	1.22	1.089	4.229 03	23.443	22.44
26	3.565	1.33	1.284	4.201 32	23.306	22.12
27	4.681	1.87	1.700	4.126 44	21.478	20.54
28	3.475	1.58	1.352	4.173 93	22.327	21.35
29	3.240	1.70	1.566	4.129 07	21.246	20.95
			1.562	4.127 86		

TABLE III. Results with probable errors, of two exponential fits, Eq. (17), to the data on lattice-parameter changes. e is the formation energy; s is the apparent formation entropy. In the first fit s is equal to zero, while in the second fit both e and s are varied.

Sample no.	Fit I ($s=0$) e (K)	Fit II e (K)	Fit II s
23	11.8±0.6	35.4±0.3	12.4±0.2
24	3.8±0.1	4.94±0.03	1.02±0.03
26	4.1±0.1	4.40±0.04	0.28±0.03
27[a]	6.8±1.3	27.16±0.02	11.78±0.01
27[b]	8.6±2.0	28.5±0.3	12.0±0.2
28	5.8±2.3	15.2±0.1	7.3±0.1
29	9.3±0.4	16.5±0.2	4.7±0.1

[a]Cooling run before phase separation.
[b]Warming run after phase separation.

molar volumes increase from 20.5 to 22.5 cm^3. (An exception is the $x=28\%$ sample no. 28 cooling data.) This qualitative tendency would not be exhibited by an analogous plot using e values from the two-parameter fits.

Note that Fig. 11 compares the NMR diffusion results with present x-ray formation data. The similarities imply (as they also do for pure bcc ^{3}He) that *migration* free energies, if any, are smaller in magnitude than the uncertainties in the respective measurements and comparison.

A compact way to illustrate the results of the two-parameter fits to present data is to plot the quantity $f=e-Ts$ versus temperature, Fig. 12. In each case f is plotted over the temperature range in which data were taken on each particular crystal. The high-temperature ends of the lines are more certain than the low-temperature ends because measurements of $\Delta a/a$ are more precise at high temperature. Qualitative inspection of Fig. 12 shows that, except for the $x=28\%$ samples, the $f(T_m)$ values fall on the same curve, regardless of mixture concentration or of molar volume. Except near its endpoints this curve lies lower than the straight $f(T_m)$ line mentioned in Sec. I, item (c).

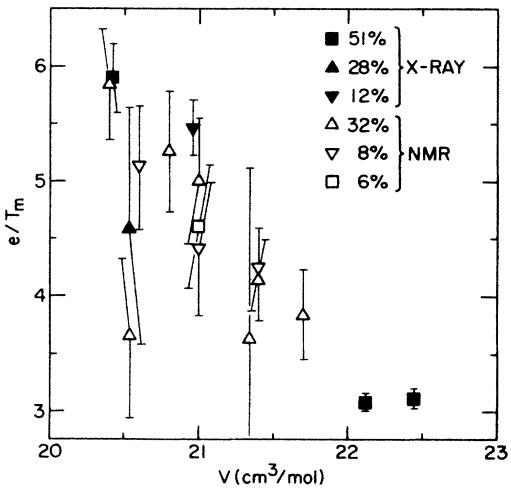

FIG. 11. Summary of current $s=0$ fits and other NMR activation energies in concentrated isotope mixtures. Plotted is a reduced energy obtained through division by the respective melting temperature. Symbols are as follows: ■, present, $x=51\%$, ▲, present, $x=28\%$; ▼, present, $x=12\%$, △, Ref. 1, $x=32\%$, ▽, Ref. 1, $x=7.8\%$; □, Ref. 2, $x=6.3\%$.

B. Vacancy entropy of formation

All the values of the parameter s (Table III) are positive (i.e., Fig. 12's slopes are negative), and some are large. From Sec. II, this does not necessarily mean that the monovacancy entropy of formation is large and positive; indeed, in a (possible somewhat ordered or inhomogeneous) concentrated mixture, there is no single definition of a monovacancy. The parameter s in a concentrated mixture represents the combined effects of vacancy binding to other vacancies and to host atoms, of ordering, and possibly of delocalization.

In usual solids the nonconfigurational monovacancy entropy at constant pressure is typically 1–2 entropy units.[12] This seems plausible from the definition

$$s_{1v}=\sum_k \ln(\omega_{km}/\omega_{kn}) , \tag{18}$$

where ω_{km} and ω_{kn} are the frequencies of the kth phonon before and after the vacancy is put into the solid. Because the vacancy allows local expansion of the lattice, the frequencies should drop when the vacancy is introduced. But under conditions of constant volume, as in solid helium experiments, the result is not so straightforward. Varotsos and Alexopoulis argue that the isochoric s is negative, when properly defined, for usual solids.[33] In

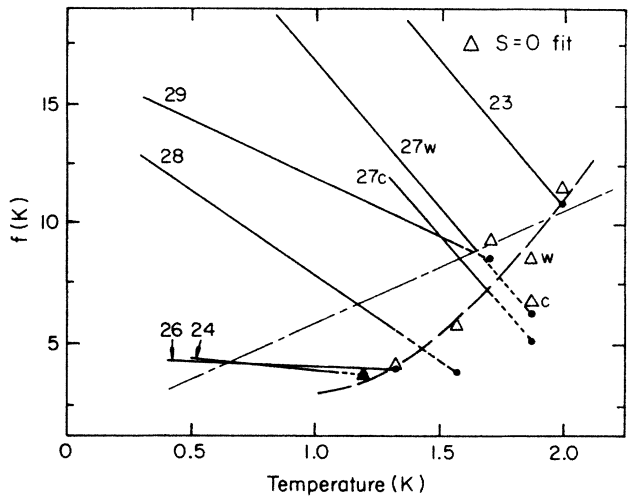

FIG. 12. Summary of free-energy results. $f(T)=e-Ts$ is plotted vs T, with values of e and s taken from the respective least-squares fits of Figs. 4–10. The solid lines extend over the temperature interval in which data were taken for each particular crystal. The short-dashed line is an extrapolation of the solid line to the observed T_m. The triangles are e values plotted at the respective T_m's for the $s=0$ fits. The long-dashed line is a guide to the eye (see text). The long-short-dashed line represents thermal vacancy results at T_m on pure bcc ^{3}He (Ref. 6) which were represented by $s=0$ fits.

pure helium, this issue has been considered by Hetherington,[34] by Widom and co-workers,[35] and by Sullivan and co-workers.[36] Hetherington concludes that $s \sim 1$ cannot be ruled out, if the vacancy is easily deformed with low-lying excited states or if it has a degenerate ground state. Widom and co-workers predict an appreciable negative entropy, but it seems to us there are inconsistencies in their assumptions, some of which are *ad hoc*. Sullivan and co-workers conclude that the contributions to s from phonons are small because $k_B T$ is always small compared to the phonon energies (frequencies) involved; they claim the only other possible contribution is the entropy associated with a lattice relaxation with less symmetry than the host lattice, which is unlikely since the energy required is larger than that for a cubic relaxation.

In order to apply quantitatively such relations as were summarized above in Sec. II, one needs vacancy-concentration data of greater accuracy than the present exploratory study provides. But one can draw some qualitative inferences. The first is that a usual assumption, that the effective s is independent of temperature, is questionable. Although a temperature-independent $s \neq 0$ is, from Figs. 4–10, consistent with the present data, the complexity of the factors contributing to the apparent vacancy concentrations does not rule out temperature dependence of the effective s_{1v}. Varotsos and Alexopolis argue that even for a monovacancy, the suitably defined s may vary with temperature.[33] The second inference follows from the observation that there are major differences in the values of the fitted s's, between mixed and pure helium crystals,[6,7] differences which depend upon molar volume, crystalline structure, or isotopic constitution. This inference is that many large contributions to the vacancy-concentration temperature dependence will have to come from vacancy binding energies and similar sources if s_{1v} is indeed zero or negative.

C. Vacancy binding effects

An upper limit of the effect of divacancies alone on the present measurements can be found by setting the divacancy binding energy e_{2b}, Eq. (3), equal to e_{1v}. Then in the approximation of Eq. (4), $\Delta N/N = -3\,\Delta a/a = 9c_{1v}$, which is simply equivalent to an increase in the contribution to the fitted entropy of $\ln(9) = 2.2$. We note that the approximation is subject to possible hazards of different contributions of entropy changes like those mentioned in the preceding section for monovacancies.

Bound states of vacancies and host atoms are another factor which can contribute to the observed changes $\Delta a/a$. A model for the free energy to be minimized is given in Sec. II, Eqs. (5)–(10). But for the concentrated isotope mixtures of the present measurements, themselves of somewhat limited accuracy, the full expression cannot be simplified without recourse to considerable assumptions. We have seen above in Sec. V A that in some sense the present $x = 28\%$ results do not fit a pattern, so let us consider just Eq. (11) in relation to the $x = 12\%$ data. The consideration is only illustrative, since 12% is, strictly, far too much for Eq. (11) to apply, since it simplifies essentially to $\exp[-(f_{1v} - f_b)/k_B T]$. From Ref. 16, the binding of a vacancy-^{3}He in a ^{4}He matrix is given as 0.2 K. If this value is attributed to the energy, not the entropy, then the results shown in Fig. 10 suggest that, since the entropy in a pure solid is likely one entropy unit or less, there is a vacancy-^{3}He binding entropy of several entropy units.

D. Vacancies in an ordered lattice?

The defect population in a partially ordered crystal is modeled by Eqs. (12)–(15). Equation (14) has an exponential character with respect to temperature, and the present data for $x = 51\%$ crystals nos. 24 and 26 clearly do too. The model applies, however, to a binary crystal in which the sign of the interaction energy w [Eq. (13)] favors unlike atoms being adjacent. This is evidently not applicable to helium isotope mixtures, at least at low temperatures where entropy contributions to the free energy are small, since these mixtures exhibit isotopic phase separation. Indeed, from regular solution theory and the measured characteristics of the coexistence curve, the low-temperature value of w is near 0.75 K for the molar volumes considered here.[11,19]

Are the possible values for e_{33}, e_{44}, and e_{34} and the apparent activation energy of about 4.5 K (Table III) incompatible? Probably not. However, few theoretical estimates of the interaction energy have been made. An early one is by Klemens and co-workers[37] and a more manifestly quantum-oriented one by Mullin.[32] Neither considered a possible temperature dependence of w. The exponent in Eq. (14) is $e_{33} - w$. That is, w needs only to have barely crossed over the range $e_{33} - 4.5$ K to produce at least partial ordering in the vacancy regime. At present, no superlattice diffraction evidence of high-temperature ordering in helium isotope mixtures has been reported. The present x-ray work could not have detected it directly, owing to similarity in the ^{3}He and ^{4}He structure factors.

From the observed cohesive energies of the pure isotopes at this molar volume, $|e_{44}| < |e_{33}|$, so that one attributes the large $3\,\Delta a/a$ value to vacancies mostly formed on the ^{4}He sites of the (speculative) ordering lattice. Qualitatively, in this model there are so many more thermal vacancies present in the (partially ordered) alloy than in a pure crystal because of the additional disorder introduced by the presence of vacancies and antisite atoms in the otherwise ordered lattice.

Another phenomenological route to numerical comparison might use defect data; within the nearest-neighbor bond-energy model, the energy to form a vacancy in a pure crystal is just a one-half the bond energy times z. For a bcc molar volume near 21 cm^3, one has a vacancy energy of about 11 K in pure ^{3}He (Ref. 6) and of about 9 K in pure ^{4}He (Ref. 7). Because of the great differences in vacancy-relaxation energies in these two cases,[7] however, it seems that use of this bond approximation would be less instructive.

In this model the considerably larger activation energy (~ 12 K) seen in the $x = 51\%$ sample no. 23 at a much smaller molar volume could mostly reflect raising of the energy per atom through compression to this volume

($PV \sim 13$ K, compared to half that value for sample nos. 24 and 26). There is known to be considerable dependence of the vacancy energy upon molar volume in pure helium.[6] Or, since in this case the measured value of $\Delta a/a$ is not so astonishing at the melting temperature, the compression could have altered the balance of w so that it did not induce high-temperature isotopic ordering at this smaller volume after all. This speculative alternative could be favored since in this case the apparent entropy is very large compared to those seen in the low-pressure 51% crystals.

E. Vacancy volumes of formation

In this section we again attribute the measured $\Delta a/a$ changes to thermal vacancy formation. In Fig. 12 dotted endpoints show the values, at melting, of $f(T_m)$. Corresponding values of V can be calculated from Eq. (16). Then application of Eq. (2) yields an estimate of the formation volume of the supposed vacancies in the population (whatever that population is in detail). The results, which apply to the respective average total vacancy populations, are shown in the last column of Table IV. For samples with $x = 28\%$, the free volume is similar to the values obtained in a variety of ways[6] in pure bcc ^{3}He. For samples with $x = 51\%$, the values appear to be about twice as large; namely, about one atomic volume.

Because for isotopic mixtures there are no comprehensive measurements of compressibility, its volume variation, and of thermal-expansion coefficient, we are unable to check the free volume of formation in the way it was done for pure ^{3}He. We do note, however, that a free volume near one atomic volume, and the corresponding pressure of vacancy formation, yields an expected pressure decrease, as the temperature is reduced from the solidus, qualitatively as large as that shown by Tedrow and Lee[38] in an $x = 78\%$ sample. (They attributed that pressure decrease to passage of their sample from liquidus to solidus, but our present measurements show presence of the solid throughout the temperature interval.) Similar large pressure changes in concentrated mixtures were seen in early measurements by Zinov'eva.[39]

TABLE IV. Inferred vacancy volumes of formation. The ratio of the vacancy volume of formation v_p to an atomic volume v_a is listed as obtained from the ratio $\Delta f/\Delta V$, volume dependence of x-ray f, in concentrated isotope crystals. For comparison, the range of deductions is shown for thermal vacancies in pure ^{3}He. For the latter case, thermodynamic data are available to make model estimates, which agree with the deductions from measurements.

Sample no.	x	V_0 (cm^3/mol)	$\Delta f_v/\Delta V$
23	0.51	20.945	1.0
24	0.51	23.443	
26	0.51	23.306	
27	0.28	21.478	0.4
28	0.28	22.327	
Ref. 6	1.0	20–24	0.5–0.4

F. Mixture molar volumes

Table IV also shows a comparison of V_0, the low-temperature x-ray molar volume, with V_m, the value calculated from Eq. (16), and the data of Grilly along the respective pure isotope melting lines.[31] On the reasonable assumption that our specimen cell did not significantly deform as the temperature was changed for a given sample,[6] each of the measurements shown in Figs. 4–10 was made along an isochore corresponding to V_0. One would then expect that for each sample the two values of molar volume would agree. For pure hcp ^{4}He,[40] for pure bcc ^{4}He,[7] and for $x = 99\%$ bcc samples[17] the values do indeed agree within the sum of the estimated uncertainties. But here in concentrated mixtures, when Eq. (16) is used, they do not. From Table IV it does seem that the relative difference between the two determinations, $(V_0 - V_m)/V_0$, approximately scales with the value of $\Delta a/a$ at melting.

In specimens of 30%, 45%, and 60% mixtures, examined with Mo $K\alpha$ radiation by Ehrlich,[41] smaller relative differences were found than the present differences in Table IV. We are not aware of any other direct checks which may have been made of Eq. (16). Perhaps its application needs further examination.

One x-ray cell had no means, unfortunately, for concurrent measurement of internal pressure corresponding to the lattice-parameter data reported here. Sensitive pressure measurements have shown some differences in pressure, attributed to nonequilibrium conditions upon temperature (and therefore pressure) cycling of pure solid ^{3}He samples,[42,43] or upon high-temperature annealing of dilute solid mixtures.[43] The most pessimistic conclusion one might draw would be that the scaling noted in the first paragraph of this section indicates that vacancy content is not after all very large in the present 51% crystals, and suggests that the x-ray data are dominated by deformation of the samples.

We regard it as very unlikely, however, that the large $\Delta a/a$ changes seen here in our low-density 51% crystals were simply observations of nonequilibrium conditions. The pioneering NMR work of Miyoshi and co-workers,[1] after all, found activation energies in a 32% mixture which were interpreted to correspond to a vacancy concentration of about 2% at the melting temperature. And, finally, there are remarkable parallels, for example, between our work and the 0.9-MPa pressure change seen by Tedrow and Lee[38] in their 78% sample. Their pressure change appears to be activated, like our sample no. 27 ($x = 28\%$) data, with a positive entropy term, and we calculate from our vacancy-formation pressure (Table IV) an expected 1.1-MPa change, in fairly good agreement with their observation.

VI. CONCLUSION

We have presented the results of the first use of x-ray diffraction as a tool with which to investigate the high-temperature properties of crystalline helium isotope mixtures, for fixed proportions of ^{3}He of 12%, 28%, and 51%. Apparently, thermally activated changes in lattice parameter were seen. If these be attributed to thermal

vacancy populations, then the results are (a) surprisingly large vacancy content in the low-density 51% crystal, suggesting the possibility of ordering in the host crystal at high temperature, (b) large apparent entropies of formation in 28% mixture crystals, suggesting that vacancy clusters and vacancy-^{3}He binding could be important, and (c) a derived average free volume of formation of the defects of about one atomic volume. We have summarized the framework for suitable discussion and outlined some speculative scenarios. But a number of interesting questions remain unanswered. Clearly, the present explorations using x-ray methods show that further research on crystalline concentrated isotope mixtures is desirable.[44]

ACKNOWLEDGMENTS

We are pleased to acknowledge the considerable assistance of P. R. Granfors and R. O. Hilleke. This research was supported in part by the U.S. Department of Energy (Division of Materials Science), under Contract No. DE-AC02-76ER01198.

*Present address: Department of Radiation Therapy, University of Michigan Hospitals, Ann Arbor, MI 48109.

[1]D. S. Miyoshi, R. M. Cotts, A. S. Greenberg, and R. C. Richardson, Phys. Rev. A **2**, 870 (1970).

[2]V. N. Grigor'ev, B. N. Esel'son, and V. A. Mikheev, Fiz. Nizk. Temp. **1**, 5 (1975) [Sov. J. Low Temp. Phys. **1**, 1 (1975)].

[3]A direct measurement of the atomic momentum distribution in hcp ^{4}He has been made by R. O. Hilleke, P. Chaddah, R. O. Simmons, D. L. Price, and S. K. Sinha, Phys. Rev. Lett. **52**, 847 (1984).

[4]A. R. Allen and M. G. Richards, Phys. Lett. **65A**, 36 (1978); A. R. Allen, M. G. Richards, and J. Schratter, J. Low Temp. Phys. **47**, 289 (1982); J. Schratter, A. R. Allen, and M. G. Richards, *ibid.* **57**, 179 (1984).

[5]S. M. Heald, D. R. Baer, and R. O. Simmons, Solid State Commun. **47**, 807 (1983).

[6]S. M. Heald, D. R. Baer, and R. O. Simmons, Phys. Rev. B **30**, 2531 (1984).

[7]P. R. Granfors, B. A. Fraass, and R. O. Simmons, J. Low Temp. Phys. **67**, 353 (1987).

[8]P. N. Henriksen, M. F. Panczyk, and E. D. Adams, Solid State Commun. **8**, 735 (1970).

[9]V. A. Mikheev, V. A. Maidanov, and N. P. Mikhin, Fiz. Nizk. Temp. **12**, 658 (1986).

[10]For example—Au-Cd: M. S. Wechsler, Acta Metall. **5**, 150 (1957); N. Nakanishi, K. M. Thein, and C. M. Wayman, J. Appl. Phys. **34**, 2847 (1963). Au-Zn: K. Mukherjee, D. S. Lieberman, and T. A. Read, J. Appl. Phys. **36**, 857 (1965); K. Mukherjee, *ibid.* **37**, 1941 (1966). Co-Ga: D. Berner, G. Geibel, V. Gerold, and E. Wachtel, J. Phys. Chem. Solids **36**, 221 (1975).

[11]B. A. Fraass and R. O. Simmons, Phys. Rev. B **36**, 97 (1987).

[12]C. P. Flynn, *Point Defects and Diffusion* (Clarendon, Oxford, 1972), Chaps. 2 and 7.

[13]N. H. March and J. S. Rousseau, Cryst. Lattice Defects **2**, 1 (1971).

[14]A. B. Lidiard, Philos. Mag. **5**, 1171 (1960).

[15]W. M. Lomer, in *Vacancies and Point Defects in Metals and Alloys* (The Institute of Metals, London, 1958), p. 79.

[16]D. P. Locke, and R. A. Young, J. Low Temp. Phys. **23**, 177 (1976).

[17]B. A. Fraass, P. R. Granfors, and R. O. Simmons (unpublished).

[18]S. M. Kim, Phys. Rev. B **29**, 2356 (1984).

[19]D. O. Edwards, A. S. McWilliams, and J. G. Daunt, Phys. Rev. Lett. **9**, 195 (1962).

[20]R. J. Wasilewski, S. R. Butler, and J. E. Hanlon, J. Appl. Phys. **39**, 4234 (1968); A. T. Donaldson and R. D. Rawlings, Acta Metall. **24**, 811 (1976).

[21]S. M. Kim and W. J. L. Buyers, Phys. Rev. Lett. **45**, 383 (1980).

[22]S. M. Heald and R. O. Simmons, Rev. Sci. Instrum. **41**, 316 (1977).

[23]National Bureau of Standards (U.S.) Reference Material 767, Superconducting Thermometric Fixed Point Device.

[24]M. Durieux, D. N. Astrov, W. R. G. Kemp, and C. A. Swenson, Metrologia **15**, 57 (1979).

[25]B. A. Fraass, S. M. Heald, and R. O. Simmons, J. Cryst. Growth **42**, 370 (1977).

[26]E. B. Osgood, V. J. Minkiewicz, T. A. Kitchens, and G. Shirane, Phys. Rev. A **5**, 1537 (1972).

[27]N. G. Bereznyak, I. V. Bogoyavlenskii, and B. N. Esel'son, Zh. Eksp. Teor. Fiz. **45**, 486 (1963) [Sov. Phys.—JETP **18**, 335 (1964)].

[28]C. Le Pair, K. W. Taconis, R. de Bruyn Ouboter, E. de Jong, and J. Pit, in *Proceedings of the International Conference on Low Temperature Physics—LT-9*, edited by J. G. Daunt, D. O. Edwards, F. J. Milford, and M. Yaqub (Plenum, New York, 1965), p. 234.

[29]K. N. Zinov'eva, Zh. Eksp. Teor. Fiz. **44**, 1837 (1963) [Sov. Phys.—JETP **17**, 1235 (1963)].

[30]B. A. Fraass, R. R. Granfors, R. O. Hilleke, and R. O. Simmons, Rev. Sci. Instrum. **55**, 1455 (1984).

[31]E. R. Grilly and R. L. Mills, Ann. Phys. (N.Y.) **18**, 250 (1962); E. R. Grilly, J. Low Temp. Phys. **11**, 33 (1973).

[32]W. J. Mullin, Phys. Rev. Lett. **20**, 254 (1968).

[33]P. A. Varotsos and K. D. Alexopoulis, *Thermodynamics of Point Defects and Their Relation with Bulk Properties* (North-Holland, New York, 1986).

[34]J. H. Hetherington, Fiz. Nizk. Temp. **1**, 613 (1975) [J. Low Temp. Phys. **1**, 295 (1975)].

[35]A. Widom, J. B. Sokoloff, and J. E. Sacco, Phys. Rev. B **18**, 3293 (1978).

[36]N. Sullivan, G. Deville, and A. Landesman, Phys. Rev. B **11**, 1858 (1975).

[37]P. G. Klemens, R. de Bruyn Ouboter, and C. Le Pair, Physica **30**, 1863 (1964).

[38]P. M. Tedrow and D. M. Lee, Phys. Rev. **181**, 399 (1969).

[39]K. N. Zinov'eva, Zh. Eksp. Teor. Fiz. **44**, 1837 (1963) [Sov. Phys.—JETP **17**, 1235 (1963)].

[40]P. R. Granfors, B. A. Fraass, and R. O. Simmons (unpublished).

[41]S. N. Ehrlich and R. O. Simmons, J. Low. Temp. Phys. **68**, 125 (1987).

[42]M. E. R. Bernier and G. Guerrier, Physica **121B**, 202 (1983).

[43]I. Iwasa and H. Suzuki, J. Low Temp. Phys. **62**, 1 (1986).

[44]M. G. Richards, J. Pope, P. S. Tofts, and J. H. Smith, J. Low Temp. Phys. **24**, 1 (1976).